

# Morphological indicators of solar exposure

**Reza Amindarbari**

Singapore University of Technology and Design

r.a.darbari@gmail.com

## ABSTRACT

This paper investigates the relation between the shading condition and geometrical configuration of neighborhood-scale developments. It introduces a straightforward method for measuring shadow areas casted on buildings' roofs and facades – in urban areas – using digital 3D models. Employing this method for measuring shadow areas in nine neighborhoods in Jinan, China, at six different time points on summer and winter solstices – a total of 54 sample measurements – this study develops two regression models that reveal the significant dependency of the in-shadow percentage of buildings' façade and roof areas to the building volume density (BVD) and height irregularity (HI) of the urban fabric.

**KEYWORDS:** urban form, geometrical configuration, solar exposure, shadow area

## 1. Introduction

While the current computational modeling capabilities allow for precise simulation of shadows and solar irradiations, they are complex and time consuming, which limits their applicability at the urban scale (Compagnon 2004). Thus, many studies have instead employed simple geometrical measures to capture the potential access to diffused solar irradiations or direct solar radiations (Robinson 2006). Among these geometric measures, sky view factor (SVF) and height to width ratio (h/w) of street canyons have been the most used ones (e.g. Oke 1987 and 1988, Arnfred 1982, Aida 1982, Adolphe 1999, Ratti et al. 1999, Robinson 2006). However, height to width ratio of street canyons is not measurable in all urban patterns: e.g. in fabrics with many large open spaces and single-standing buildings, such as the tower-in-park typology.

Assessment of the sky view factor is not also an easy task. The classic methods are based on on-site surveys, using fisheye lenses, which is a time consuming and expensive process. Some efforts have been made for developing computational methods of sky view factor measurement, based on either raster or vector digital

3D datasets. All the rare examples of vector-based SVF analysis methods are highly computationally demanding: for example 3DSkyView, a 3D extension to ArcView 3.2 (Souza et al., 2003), and the extension developed by Li et al. (2004) for ArcScene 8.3. Although significantly faster than vector-based methods (Gal et al. 2008), raster analysis methods, often based on digital elevation models (Ratti et al. 1999, Lindberg 2005, Gal et al. 2007 & 2008), are still highly time consuming at urban scales<sup>1</sup> and not yet available to planners who do not have a high level of programming skill.

Thus, this paper investigates whether buildings volume density and height irregularity, which are simply measurable, can be used as morphological indicators of solar exposure and shading condition. Cheng et al. (2006) have studied the impact of floor area ratio (FAR) and height irregularity on daylight factor and PV potential. Different from their work, which is based on eighteen generic models, the work presented here is based on real world urban patterns. More importantly, this work

<sup>1</sup> - In Gal et al.'s work (2008), the computation of the SVF for 7,562,500 points covering Szeged (26.75 KM<sup>2</sup>) took 38 h on a regular PC, while it would take 12 days using a vector-based method.

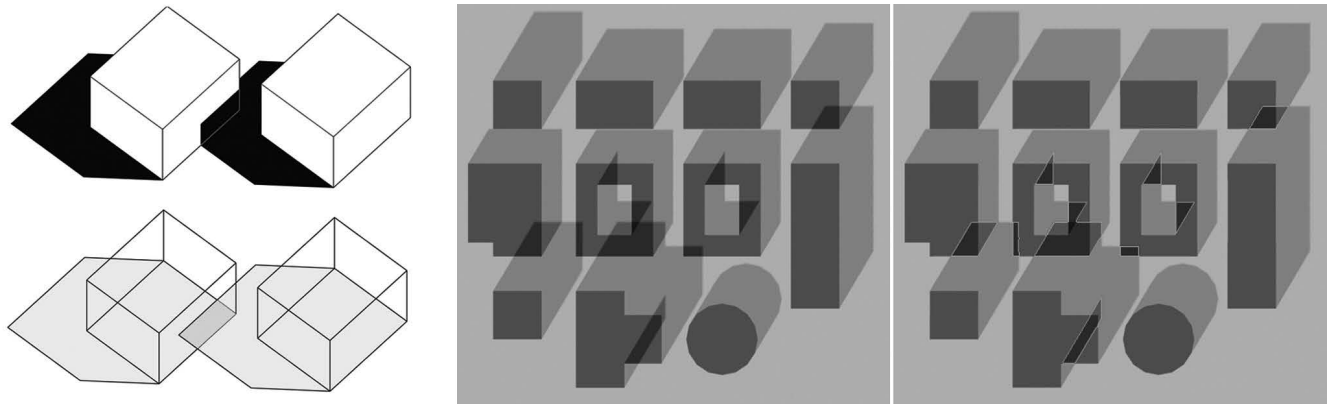


Figure 1: a) When buildings are transparent in a digital 3D model, the shadows, which were supposed to be casted on buildings' surfaces, would be projected onto the ground along the solar beams. b) Top view shadow simulation of a 3D model with transparent buildings. The projection of the in-shadow parts of roofs and facades onto the ground creates dark areas (darker than other shadows, buildings' footprint, and the ground). The marked areas are the projections of the in-shadow parts of roofs and facades onto the ground.

develops two regression models for estimating the amount of shadows casted on buildings surfaces based on these two attributes (HI and BVD).

First, a straightforward hybrid raster-vector method is introduced for measuring the area of the in-shadow parts of buildings surfaces. This method is based on the *raster* analysis of the top view renderings of the study area – with simulated shadows<sup>2</sup> – derived from the *vector* 3D model of the study area in which a uniform *transparent* material is applied to all buildings. It basically tries to measure, on neighborhoods' top-view renderings, the in-shadow areas of not only roofs but also facades.

Then, using the introduced hybrid method in nine neighborhoods in Jinan, China, the area of the in-shadow parts of buildings surfaces (roofs and facades) are measured for six different time points on summer and winter solstices – a total number of 54 samples. Finally, based on the derived shadow areas, two regression models are developed, which confirm the significant dependency of the in-shadow percentage of buildings' façade and roof areas to the building volume density (BVD) and height irregularity (HI) of the urban fabric, controlled for solar altitude.

## 2. The Measurement of the in-Shadow Areas

Several 3D modeling software tools can simulate shadows and sunlight (direct and diffused solar radiation) at any time of the day and year, and in any geographic location, and provide raster outputs. It is possible to directly measure the area of shadows on a top view (site plan) raster image through simple image processing, if it is in a known scale. However, it is not a

2 –It is assumed that shadow areas simulated by computational modeling tools (namely AutoCAD 2011 for this research) are geometrically similar to the real world situation; i.e. the area of shadows measured on computationally simulated images are exactly the same as the actual area of shadows in the real world.

trivial task when it comes to facades. When the study area constitutes a large number of buildings, it is very unlikely to capture all the in-shadow parts of all façades in a limited number of raster images, as the buildings in foreground block those located behind them.

However, if we project the in-shadow parts of facades onto the ground (plan view), visualize this projection and find the relation of the area of the projected shadows to their actual area, we can measure the area of the in-shadows parts of facades. Applying transparent materials to buildings in a 3D model allows the shadows that are casted on buildings' surfaces to be projected along solar beams onto the ground (Fig.1a), which can be distinguished from shadows that opaque buildings would have cast on the floor (Fig.1b). In the absence of diffused solar radiations, the shadow of opaque objects would be absolutely black. However, the shadow of transparent materials are not completely black, even without diffused solar radiation, as transparent buildings allows the light to pass through their volume and shadows will partially receive light. As the shadows are not absolute, when two or more shadow layers overlap, they create a darker shadow (Fig.1b).

In addition, the ratio of the area of the in-shadow fractions of facades to the area of their projection can be proved to be equal to the tangent of solar altitude (Fig. 2a). Where  $A_{SF}$  is area of shadows casted on buildings facades,  $A_{PF}$  is the area of their projection along solar beam onto the ground, and  $a$  is solar altitude, and  $L_1 = L_2 \cdot \tan(a)$ , and thus:  $A_{SF} = A_{PF} \cdot \tan(a)$ .

It should be noted that the dark shadows constitutes shadows casted both on façade and roofs – i.e. shadows casted on roofs would also be projected onto the ground and create dark shadows. But the in-shadow parts of roofs and their projection onto the ground have the same size (Fig.2b); i.e. where  $A_{SR}$  is the area of in-shadow parts of roofs and  $A_{PR}$  the area of their projection

onto the ground,  $A_{SR} = A_{PR}$ ; thus, if  $A_{TP}$  is the total area of the projection of shadows (dark shadows),  $A_{PF} = A_{TP} - A_{PR}$  and  $A_{SF} = (A_{TP} - A_{PR}) \cdot \tan(a)$ . The area of shadows casted on roofs,  $A_{SF}$ , can be simply derived from top view renderings with opaque buildings, where any shadows located within the footprint area of buildings is in fact casted on the roof.

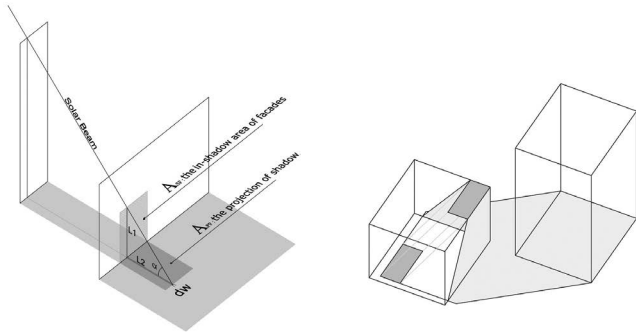


Figure 2: a) The ratio of the area of the in-shadow fractions of facades to the area of their projection on the ground is equal to the tangent of solar altitude. b) However, the area of the shadows casted on the roofs and their projections onto the ground are equal.

There are two assumptions, only under which the introduced hybrid method and the above equations would be valid:

1. The roofs are horizontal and the façade surfaces are vertical, however method can capture shadows that setbacks and cantilevers generate.
2. The ground surface is flat. Otherwise, if the site is steep, it can be shown that  $A_{SF} = A_{PF} [\tan(a) - \tan(Q)]$  where  $\tan(Q)$  is the slope of the ground. If the land site is flat, then  $\tan(Q)$  would be zero, and again  $A_{SF} = A_{PF} \cdot \tan(a)$ .

## 2.1 Surfaces in the Dark Sides of Buildings

A building's surface would be in shadow either when another surface obstructs solar radiation, or when it is in its own shadow – i.e. being located in the dark side of the building (Fig.3a). While the former, besides the position of the sun in the sky, is dependent on the configuration of the buildings in the site, the latter is independent of the urban form, and is only related to the position of the sun in the sky and the orientation of the surface. Thus, if we are interested in the impact of urban form to shading condition, the area of surfaces located in dark of sides of buildings should not be taken into account; particularly given their large amount<sup>3</sup>, they can profoundly influence the results. Thus, the shadow ratio is specified as the in-shadow percentage of only buildings' surfaces *that face the sun* and could potentially receive the solar radiation.

The introduced hybrid method measures only the area <sup>3</sup> - For example, in equiangular polygons with even number of edges (e.g. squares and rectangles), and in circles, 50% of the area of facades are always in the dark side of the building

of shadows casted on surfaces, which are not in dark sides of the building, and could potentially receive the solar radiation, but may be obstructed by other surfaces. To calculate the shadow ratio of these surfaces – as specified above – it is only required to differentiate facades that face the sun, and measure their area. As shown in figure 3b, a facade would face the sun, only if the angle between its normal vector – directed from inside to outside of the building – and solar azimuth is larger than 90 degrees.

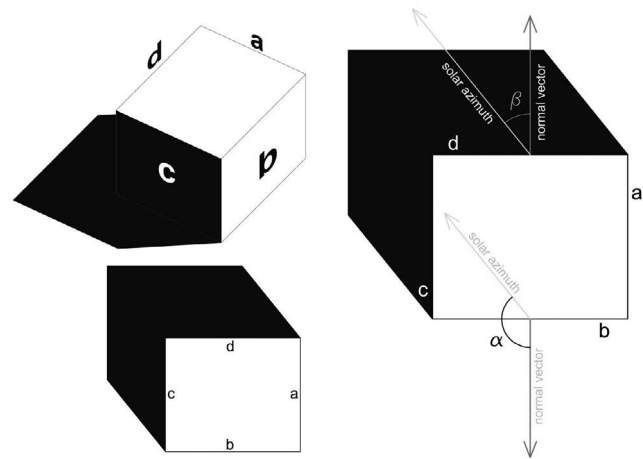


Figure 3: a) Façade c is in the dark side of the building or in fact in its own shadow. b) Angle a, the angle between solar azimuth and the normal vector of the façade is greater than 90° and the façade faces the sun, but angle b, is less than 90° and this façade is in the dark side of the building.

## 3. Geometric Indices

### 3.1 Building Volume Density

The closer the buildings are, the higher the chance that they cast shadow on each other is. In this work, the compactness of urban fabric is specified as their building volume density. For a neighborhood, building volume density is the ratio of the total volume of buildings to the total volume of the neighborhood, which is equal to the sum of the volume of open spaces and buildings. The volume of open spaces is defined as the area of open spaces multiplied by the weighted average height of the buildings – the average is weighted based on the area of buildings footprint. The area of open spaces is derived from the subtraction of buildings footprints from the site area. The convex hull polygon<sup>4</sup> of the buildings is used as a consistent way of defining the site area.

### 3.2 Height Irregularity

When buildings have the same height, they can't cast shadow on each others' roof. Conversely, the higher the height irregularity is, the higher the chance that

<sup>4</sup> - The smallest concave polygon that fully contains all individual polygons of the urban extent of a city

buildings cast shadow on each others' roof, is. Height irregularity is calibrated as the standard deviation of buildings height relativized by the area of buildings footprint.

#### 4. Case Studies: Analysis And Results

Nine neighborhoods in Jinan, China, are used for studying the urban-form/shading-condition correlation. These neighborhoods represent four distinct typologies: a) traditional neighborhoods with 1-3 story courtyards and fractal fabric b) grid neighborhoods which mainly built in 1920's with a grid block pattern and various building forms c) enclaves often developed in 80's and 90's with linear mid-rise buildings and finally d) superblocks (aka towers in park) mainly developed after 2000.

The two geometric indices, height irregularity (HI) and building volume density (BVD), are measured (table 1) for these neighborhoods in ArcMap 10, using their GIS building polygon maps and buildings' height information.

	Foshan-Yuan	Dong-Cang	Lv-Jing	Old Commercial	Shanghai Garden	Wuying-Tan	Sunshine 100	Yanzi-Shan	Zhang Village
BVD	0.38	0.36	0.28	0.30	0.22	0.28	0.14	0.33	0.54
HI	3.20	3.50	5.80	8.45	6.04	2.50	17.06	6.04	0.94

Table 1: Height Irregularity (HI) and building volume density (BVD) of the nine neighborhoods

Using the introduced shadow measurement method, the amount of shadows on facades and roofs are measured at 10:30, noon and 13:30 of summer and winter solstices. The top view images of the nine neighborhoods with transparent buildings, derived in AutoCAD 2011, are processed in Adobe Photoshop (Fig.4b); dark shadows are selected and filled with black, while the other parts of images are filled with white(Fig.4c), and the mode of images is changed to "Indexed Color", to be convertible to polygon shape files in ArcMap 10, to measure their areas. Likewise, the area of shadows casted on rooftops is also measured.



Figure 4: a) top view of Yanzi-Shan with transparent buildings at 10:30 December 21; b) marked areas are the dark shadows, c) the map of dark shadows (projection of shadows casted on buildings' surfaces) generated in Adobe Photoshop.

Based on the coordinates of the start and end point of buildings edges (in the plan), the orientation of facades and their normal vector is obtained in ArcMap. For the six mentioned times on the summer and winter solstices, façades that face the sun are determined and their total area is calculated. Finally, the shadow ratio for facades and roofs of the nine case neighborhoods are calculated for these times total 54 observed samples.

The first hypothesis is that the shadow ratios of facades are directly related to the building volume density and negatively to the solar altitude; i.e. the higher amount of shadow is expected in compact clusters. In addition, when the sun is at a higher altitude, the shadows would be obviously shorter, thus we expect  $R_{SF} = K_1 \times BVD / \tan(a)$  or  $R_{SF} = K_1 \times BVD / \tan(a)$  ( $K_1$  is a constant). The analysis confirms this hypothesis (Fig.5a). The second hypothesis is that the shadow ratio of roofs is proportional both to BVD and height irregularity, and inversely related to the solar altitude; i.e.  $R_{SR} = K_2 \times HI \times BVD / \tan(a)$  or  $R_{SR} = K_2 \times HI \times BVD / \tan(a)$  ( $K_2$  is a constant). The regression analysis confirms this hypothesis as well (Fig. 5b). Based on the regression results  $K_1$  is 0.475 and  $K_2$  is 0.0165:

(for facades) and (for roofs)

#### 5. Conclusion

The analysis confirms that building volume density (BVD) and height irregularity (HI) can be used as indicators of the shading condition in the urban fabric. The importance of these two geometric attributes lies in the simplicity of their calculation, as they can be measured only based on buildings' height and footprint area, and total site area.

#### Acknowledgment

I would like to gratefully acknowledge the enthusiastic supervision of Professors Dennis Frenchman and Christopher Zegras, the co-principal investigators of the Making the Clean Energy City in China research. I would also acknowledge the support from the Energy Foundation for this work as a part of the Making the Clean Energy City in China research, conducted at MIT Department of Urban Studies and planning, in partnership with Tsinghua University.

#### References

- Adolphe, L. 2001. A Simplified Model of Urban Morphology: Application to an Analysis of the Environmental Performance of Cities. *Environment and Planning B: Planning and Design*, 28, 183-200
- Aida, M.1982. Urban albedo as a Function of the Urban Structure: a model experiment. *Boundary-Layer Meteorology*,23,405-414
- Arnfeld, A.J. 1982. An Approach to the Estimation of the Surface Radiation Properties and Radiation Budgets of Cities. *Physical Geography*, 3, 97-122
- Cheng, V. Steemers, K. Montavon, M. and Compagnon R. 2006, Urban Form, Density and Solar Potential. *Proceeding of The 23rd Conference on Passive and Low Energy Architecture PLEA2006*, Geneva, Switzerland
- Compagnon, R. 2004. Solar and Daylight Availability in the Urban Fabric. *Energy and Buildings*, 36, 321-328
- Evans, M. 1980, Housing, Climate and Comfort. *The Architectural Press*, London

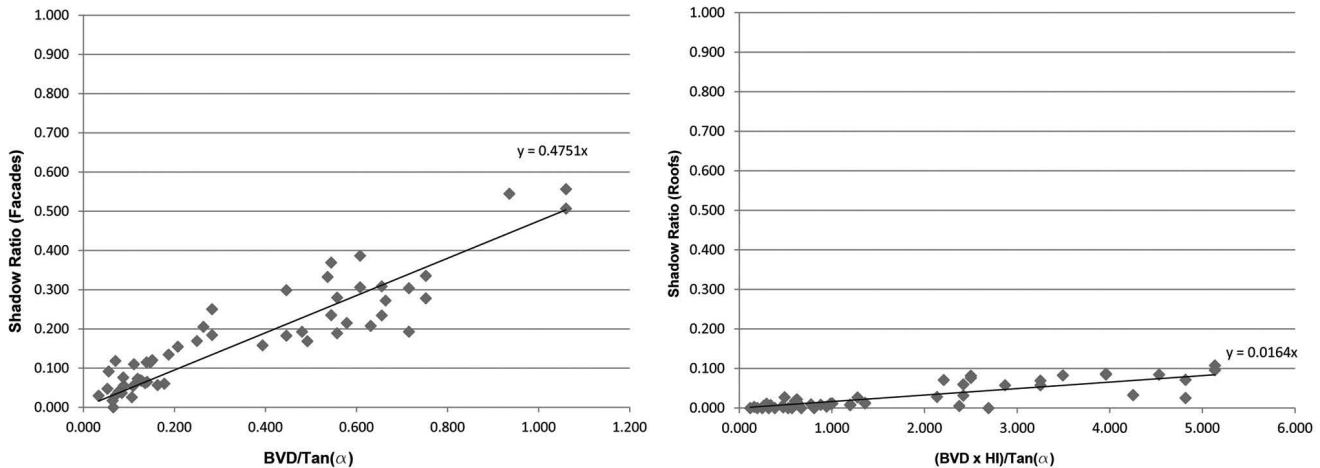


Figure 5: a) Facades' shadow ratio is directly related to building volume density (BVD) and negatively to the solar altitude (a).  $R^2$  is 94%, and P-value 0.0000 b) The shadow ratio of roofs is proportional both to building volume density (BVD) and height irregularity (HI), and inversely related to the solar altitude (a).  $R^2$  is 80%, and P-value is 0.0000.

Ga' l, T. Lindberg, F. Unger, J. 2008. Computing Continuous Sky View Factors Using 3D Urban Raster and Vector Databases: Comparison and Application to Urban Climate. *Theoretical and Applied Climatology*, 95, 111–123

Gal T. Rzepa M. Gromek B. Unger J. 2007. Comparison between Sky View Factor Values Computed by Two Different Methods in an Urban Environment. *ACTA Climatologica Et Chorologica*, 40(41), 17–26.

Li, W. Putra, S. Yang, P. 2004. GIS Analysis for the Climatic Evaluation of 3D Urban Geometry: the Development of GIS Analytical Tools for Sky View Factor. *Proceeding of the Seventh International Seminar on GIS in Developing Countries (GISCO)*, Universiti Teknologi Malaysia, Skudai, Johor, Malaysia

Lindberg F. 2005. Towards the Use of Local Governmental 3D Data within Urban Climatology Studies. *Mapping Image Science*, 2, 32–37

Oke, T.R. 1987. *Boundary Layer Climates*, Routledge, London.

Oke, T.R., 1988: Street Design and Urban Canopy Layer Climate. *Energy and Buildings*, 11, 103-113.

Ratti, C. Raydan, D. Steemers, K. 2003. Building form and environmental performance: archetypes, analysis and an arid climate. *Energy and Buildings* 35, 49–59.

Ratti, C. Richens, P. 1999. Urban Texture Analysis with Image Processing Techniques. *Proceedings of CAAD Futures 99*, Atlanta

Robinson, D., 2006. Urban Morphology and Indicators of Radiation Availability. *Solar Energy*, 80, 1643–1648.

Souza, L. Rodrigues, D. Mendes, J. 2003. A 3D-GIS Extension for Sky View Factors Assessment in Urban Environment. *Proceeding of the International Conference on Computers in Urban Planning and Urban Management (CUPUM'03)*, Sendai, Japan.